



## Research article

# Application of multi-model switching predictive functional control on the temperature system of an electric heating furnace



Weide Xu, Junfeng Zhang, Ridong Zhang\*

Key Lab for IOT and Information Fusion Technology of Zhejiang, Information and Control Institute, Hangzhou Dianzi University, Hangzhou 310018, PR China

## ARTICLE INFO

## Article history:

Received 20 July 2016

Received in revised form

9 January 2017

Accepted 1 February 2017

Available online 7 February 2017

## Keywords:

Industrial electric heating furnace

Predictive functional control

Multi-model switching systems

## ABSTRACT

A method of multi-model switching based predictive functional control is proposed and applied to the temperature control system of an electric heating furnace. The control strategies provide the effective and independent control modes of the electric heating furnace temperature in order to obtain improved control performance. The method depends on conventional implementation of the multi-model switching state, which requires some endeavors to tune the switching model in the model predictive control and allows a reduction of the calculation compared with the weighted multiple model algorithms. In order to test the advantage of the proposed method, experimental equipment is set up and experiments are done on the temperature process of a heating furnace, which verify the validity and effectiveness of the proposed algorithm.

© 2017 ISA. Published by Elsevier Ltd. All rights reserved.

## 1. Introduction

Electric heating furnace is a kind of equipment that is widely used in industrial processes [1]. It is characterized with large inertia, time delay and uncertainty and it is very hard to obtain high control precision by traditional control methods. The performance of electric heating furnace has a direct impact on the efficiency of the subsequent product, so it is important to find effective control methods.

Proportional-integral-derivative (PID) control algorithm is the most commonly used method in industry [2]. Most researchers have been directed towards the PID design so far in the process control field, primarily because the algorithm is easily implemented with acceptable performance. However, the control system's speed and overshoot are affected by the control parameters and how to adjust these parameters is the key issue that influences the performance of the control system. Some papers have been published to present different control strategies for tuning the parameters of PID. In [3], a method for adjusting the parameters of the PID controller based on the steady state characteristic and the stability margin of the feedback closed loop system is proposed. Internal model control (IMC) schemes are common in this field and usually involve the use of a model to form an equivalent PI controller [4]. However, PID control algorithms can hardly meet the situation that industrial processes are becoming more and more complex with large inertia and time delay.

Nowadays, model predictive control (MPC) is seen as a promising alternative to typical control schemes like PID [5–8]

because it can effectively deal with industrial processes with uncertainty. MPC cascade feedback control has also been proposed for the control of chemical industrial furnace in different fields [9–11]. The authors in [12] present an application of nonlinear MPC with a dead time compensator to control a distributed solar collector. An input-output feedback linearization scheme for doubly-induction generators has been proposed in [13]. In [14], the authors investigated MPC schemes for a reactive distillation column used for the hydrogenation of benzene. MPC in precision tracking control and constraint handling of mechatronic servo systems is proposed in [15]. In [16], a MPC scheme for industrial coke fractionation tower was presented. The control algorithm is a kind of MPC cascade control that the inner P control system is treated as a new state space model for MPC design.

In spite of its advantages, the classical implementation of MPC also suffers from some disadvantages, namely the insufficient precision of offline identified modes in the nonlinear system. Hence, the phenomena of delay, large inertia and time varying of parameters in the process should be considered not only in the control algorithm but also in the mathematical models. In nonlinear systems, the dynamic response of the process is ultimately limited by the model precision. Moreover, some efforts have to be made to develop new modeling approaches in order to improve the accuracy of the process model [17].

Multiple model control strategy is effective for processes with strong nonlinearity and time-varying parameters [18,19]. In [20], a switching multi-model predictive control strategy is used for hypersonic vehicle with strong nonlinearity. In [21], the authors proposed multiple models combined with Bayes theorem to describe the nonlinear hybrid systems. In [22], a multiple-model

\* Corresponding author.

E-mail address: [zrd-el@163.com](mailto:zrd-el@163.com) (R. Zhang).

predictive control strategy for the component content in the rare earth extraction process is discussed. It's no doubt that we can effectively combine MPC with the multiple models to deal with the large inertia phenomenon and nonlinearity issues in the processes [23–25].

Motivated by the above-mentioned situation, the main contribution of this paper is to propose a multi-model switching based predictive functional control (PFC) method to cope with the nonlinearity and uncertainty of industrial processes. In this paper, the multi-model switching based PFC algorithm is first designed and then implemented on the temperature process of a SFX-40 electric heating furnace. The main contributions of this paper are as follows:

- (1) Implement the inner PI control in the temperature loop to form a PI control system.
- (2) Divide the working conditions into several submodels to increase the modeling precision.
- (3) Design the multi-model switching PFC for the local models to increase the overall performance.

This paper is organized as follow. In Section 2, the process modeling and the multi-model switching based on predictive functional control method are introduced. In Section 3, the experimental setup, the system hardware, software and the temperature process are described. In Section 4, experiment results of implementing the proposed algorithms on the temperature of the electric heating furnace are shown. Finally, conclusion is given in Section 5.

## 2. Mathematical models and the PFC control algorithm

### 2.1. Process model

The implementation of modeling requires large amounts of data, which is the first step in the controller design. For convenience of the subsequent controller design, a typical first order plus dead time (FOPDT) model is adopted here.

$$G(s) = \frac{y(s)}{u(s)} = \frac{K}{Ts + 1} e^{-\tau s} \quad (1)$$

where  $G(s)$  is the Laplace transform of the process model,  $y(s)$  and  $u(s)$  are the Laplace transforms of the process output  $y(t)$  and input  $u(t)$ , respectively.  $K$  is the steady process gain,  $T$  is the time constant and  $\tau$  is the time delay.

Identification of the three parameters is the key step in process modeling. The process output change divided by the input change can be calculated to obtain the process gain. The delay and the time constant are estimated by the two-point method in the literature [26]. The response of  $y(t)$  to the step input is

$$y(t) = \begin{cases} 0 & , t < \tau \\ K - Ke^{-\frac{t-\tau}{T}} & , t \geq \tau \end{cases} \quad (2)$$

Denote  $y(\infty)$  as the steady value of  $y(t)$  and  $U$  as the input step signal change. The steady process gain  $K$  is then calculated as  $K = \frac{y(\infty) - y(0)}{U}$ .

The typical two different time points  $t_1$  and  $t_2$  are chosen such that

$$\begin{aligned} y(t_1) &= 0.39(y(\infty) - y(0)) + y(0) \\ y(t_2) &= 0.63(y(\infty) - y(0)) + y(0) \end{aligned} \quad (3)$$

Then the time constant  $T$  and the delay  $\tau$  are derived as follows:

$$\begin{aligned} T_1 &= 2(t_2 - t_1) \\ \tau_1 &= 2t_1 - t_2 \end{aligned} \quad (4)$$

### 2.2. Predictive functional control design

Firstly, the model of the process without the delay part will be considered as follows:

$$G(s) = \frac{y(s)}{u(s)} = \frac{K}{Ts + 1} \quad (5)$$

Based on the sampling time of  $T_s$ , the discrete model of the process is expressed as:

$$y_m(k) = a \cdot y_m(k-1) + K \cdot (1-a) \cdot u(k-1) \quad (6)$$

where  $a = e^{-\frac{T_s}{T}}$ ,  $y(k)$  and  $u(k-1)$  are the discrete output variable and input variable of the process model at corresponding time instants, respectively.  $k$  is the current time instant.

According to the above prediction model, the future  $H$  step predicted value of the model can be calculated by the current model output value  $y_m(k)$  and control input  $u(k)$  under the condition that  $u(k) = u(k+1) = \dots = u(k+H-1)$ :

$$y_m(k+H) = a^H \cdot y_m(k) + K_m \cdot (1 - a_m^H) \cdot u(k) \quad (7)$$

For the above process model, we choose the following first order reference trajectory:

$$y_r(k+H) = y_p(k) + (c - y_p(k)) \left[ 1 - e^{-\left(\frac{H \cdot T_s}{Tr}\right)} \right] \quad (8)$$

where  $y_p(k)$  is the process output,  $Tr$  is the time constant of the reference trajectory.

In order to improve the robustness of the control system, the error feedback correction is introduced as follows:

$$y_m(k+H) + e(k) = y_r(k+H) \quad (9)$$

where  $e(k)$  is the deviation of the model output and the actual output at the time instant  $k$ :

$$e(k) = y_p(k) - y_m(k) \quad (10)$$

Consider the following objective function:

$$J = \min (y_m(k+H) + e(k) - y_r(k+H))^2 \quad (11)$$

then the input control of the current instant can be obtained as:

$$u(k) = \frac{(c - y_p(k)) \cdot (1 - \beta^H) + y_m(k) \cdot (1 - a_m^H)}{K_m \cdot (1 - a_m^H)} \quad (12)$$

Now, consider the time delay in the process, the difference equation is expressed as:

$$y(k) = a \cdot y(k-1) + K \cdot (1-a) \cdot u(k-d) \quad (13)$$

where  $d = \frac{\tau}{T_s}$ .

By reference to the idea of Smith predictor, we use a process model with no delay time to correct the measured process output values. The process output of the controlled process is:

$$y_p(k) = a \cdot y_p(k-1) + K \cdot (1-a) \cdot u(k-1-d) \quad (14)$$

The process output of the model with delay is:

$$y_m(k) = a \cdot y_m(k-1) + K \cdot (1-a) \cdot u(k-1-d) \quad (15)$$

Since the process model output without time delay is expressed as:

$$y_{\text{mav}}(k) = a \cdot y_{\text{mav}}(k-1) + K \cdot (1-a) \cdot u(k-1) \quad (16)$$

the output of the revised process is compensated for as:

$$y_{\text{pav}}(k) = y_p(k) + y_{\text{mav}}(k) - y_{\text{mav}}(k-d) \quad (17)$$

where,  $y_{\text{mav}}(k)$  represents the output of the model when there is no delay in the system,  $y_m(k)$  represents the output of the model when delay exists in the system,  $y_{\text{pav}}(k)$  represents the output of the model after the delay compensation.

From Eqs. (12), (16) and (17), the input control of the process can then be obtained as:

$$u(k) = \frac{(c - y_{\text{pav}}(k)) \cdot (1 - \beta^H) + y_{\text{mav}}(k) \cdot (1 - a_m^H)}{K(1 - a_m^H)} \quad (18)$$

### 2.3. Module switch

Due to the fact that the process parameters are time varying as the temperature continues to rise, here the dynamics of the process will be represented with several models that belong to different zones according to the temperature and time. In order to improve the accuracy of the control performance, the model in the corresponding zone will be adopted as the process model. For simplicity, if the temperature exceeds current time zone and will reach the next zone, we will directly switch the current model to the model in the next zone for controller calculation. The accuracy of the model will directly affect the performance of the predictive control. In order to improve the accuracy of the control performance and obtain a more accurate model under different working conditions, the system can be switched at different temperatures in order to get a better control system. When the temperature reaches the temperature of the current working model, the system should adjust the corresponding working model for improved control performance.

## 3. Experiment equipment

The temperature process control system of the electric heating furnace consists of three parts, which are the temperature acquisition system, industrial processing computer (IPC) and the contactor relay for heating. The implementation procedure of this equipment is depicted in Fig. 1.

### 3.1. Temperature acquisition system

In the temperature measurement part, the function of the thermocouple is to measure the temperature. Through measuring the temperature in the furnace, the thermocouple generates a voltage difference signal between the two output poles and sends it to the signal amplifier SG-3011CR to be amplified. This amplified signal will then be sent into the PCI-1802LU CR signal acquisition card. The signal acquisition card PCI-1802LU CR then transforms this voltage difference signal into digital signal for further use in the processing unit of industrial processing computer.

### 3.2. Industrial processing computer

Industrial processing computer (IPC) is an intermediate part that connects the signal acquisition card PCI-1802LU CR and the SSR-380D40 solid state relay. It receives the data from PCI-1802LU CR and calculates the heating time of the solid state relay through the predesigned control algorithm for the temperature system. The control algorithm is implemented with the C programming

language, which is one of the most popular programming languages. The heating time signal is a digital signal and will be transformed into the corresponding voltage signal through PIO-D24U signal output card.

### 3.3. Solid state relay

The heating time for the furnace temperature is implemented by the SSR-380D40 solid state relay, which transforms the corresponding voltage signal to the on-off state signal. When the output of the IPC is  $0 \times 01$ , the PIO-D24U signal output card will produce +5 V output signal for the SSR-380D40 solid state relay. The SFX 4–10 electric heating furnace is then on the heating state. On the contrary, if the output signal of the IPC is  $0 \times 00$ , the voltage of PIO-D24U signal output card will be 0 V, then the SFX 4–10 electric heating furnace is not on the heating state.

## 4. Experiment results

### 4.1. System identification

The step-response test is done to obtain the temperature dynamics. Here the process data are gathered every 10 s and the duty cycle of 20% is set. This duty cycle is kept fixed until the temperature data maintain unchanged or change slowly indicating the process has reached the steady state. The response of the process is shown in Fig. 2.

Based on two-point modeling method, the process model is expressed as follows:

$$G(s) = \frac{28.5}{735s + 1} e^{-10s} \quad (19)$$

The delay can be obtained by Pade approximation, then the transfer function is described as:

$$G(s) = \frac{Ke^{-\tau s}}{Ts + 1} = \frac{K(-0.5\tau s + 1)}{(Ts + 1)(0.5\tau s + 1)} \quad (20)$$

This transfer function is then separated into two different parts, the stable parts  $G_{p-}(s) = \frac{K}{(Ts + 1)(0.5\tau s + 1)}$  and unstable part  $G_{p+}(s) = -0.5\tau s + 1$

Thus the IMC controller can be described as:

$$q(s) = \frac{1}{G_{p-}(s)} f(s). \quad (21)$$

The equation of internal model control and PID control can be obtained:

$$u(s) = \frac{q(s)}{1 - G_{p+}(s)f(s)} = \frac{1}{K} \frac{(Ts + 1)(0.5\tau s + 1)}{(\lambda + 0.5\tau)s} \quad (22)$$

$$u(t) = k_p \left[ e(t) + \frac{k_i}{k_p} \int_0^t e(t) dt + \frac{k_d}{k_p} \frac{de(t)}{dt} \right] \quad (23)$$

According to IMC-PID, the parameters can be calculated by the formula:

$$k_p = \frac{(T + 0.5\tau)}{K(\lambda + 0.5\tau)}, \quad k_i = \frac{k_p}{T + 0.5\tau} \quad (24)$$

Based on IMC,  $\lambda$  should be more than  $0.8\tau$ . However, to let PID yield a relative fast response, we finally choose  $\lambda = 4.5$ . The parameters of P and I can then be achieved as 2.74 and 0.0037 respectively by the above equations. The IMC control structure is shown in Fig. 3.

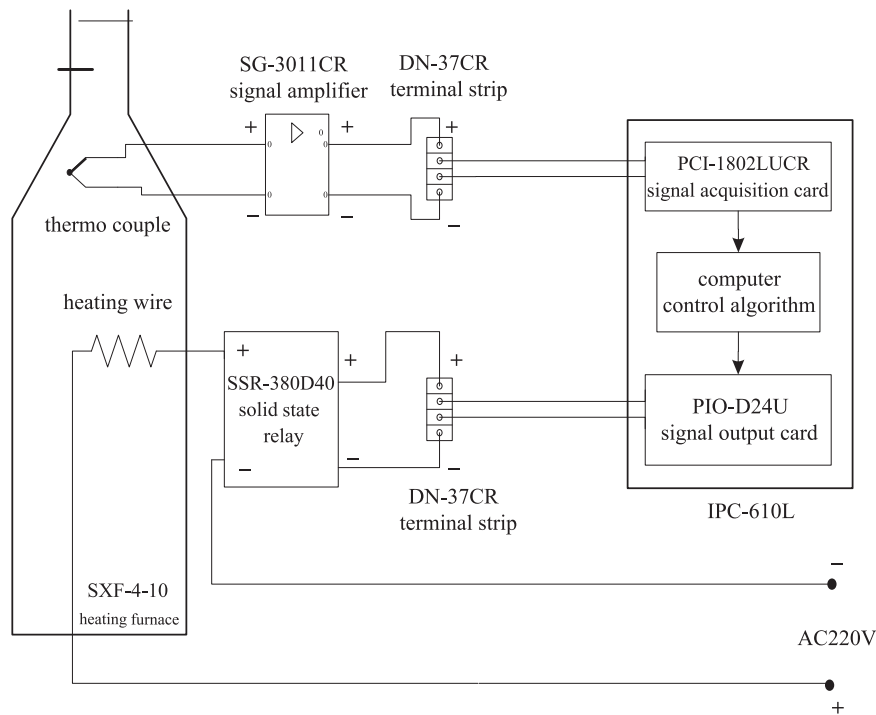


Fig. 1. The electric heating furnace SXF-4-10.

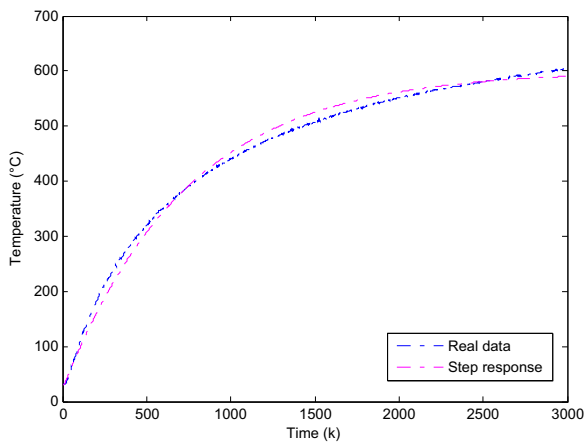


Fig. 2. Step response of the furnace process.

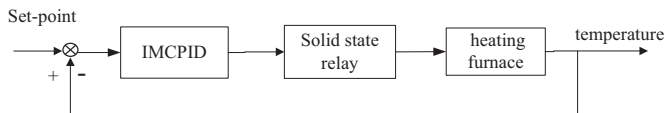


Fig. 3. The structure of the IMCPID.

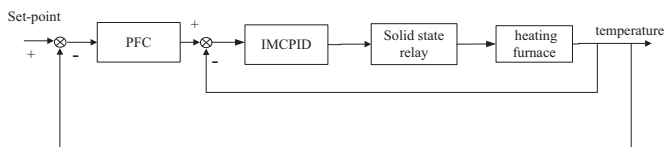


Fig. 4. The structure of the PFC-PID.

The closed-loop system is depicted as follow:

The PID closed-loop system will then be viewed as a generalized process and modeled for further PFC controller design, which is shown in Fig. 4.

#### 4.2. Multiple models

Here the objective temperature is 300 °C and it will be divided into two sections on average. The first section of the temperature ranges from 0 °C to 150 °C, and the second section of the temperature ranges from 150 °C to 300 °C. The models for the two sections can be obtained by arrange the set-point of the PID controller as 150 °C and 300 °C respectively. Based on the two-point method, we can get the parameters of the two section models.

When the temperature set-point is changed to 150 °C, the first order plus dead time model based on the step response shown in Fig. 5 is modeled as:

$$G(s) = \frac{1}{520s + 1} e^{-100s}$$

When the temperature set-point is changed from 150 °C to 300 °C, the first order plus dead time model based on the step response shown in Fig. 6 is modeled as:

$$G(s) = \frac{1}{1100s + 1} e^{-100s}$$

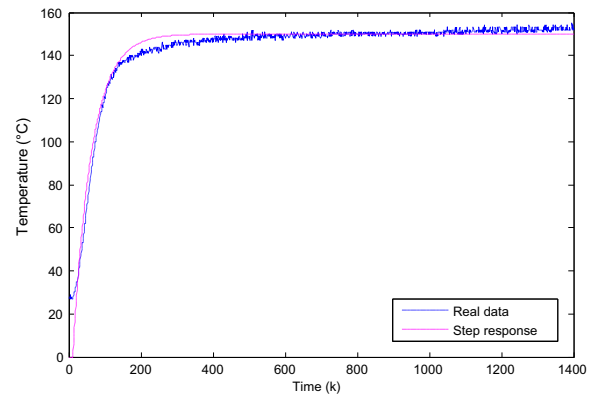


Fig. 5. Step response of the generalized process under the temperature set-point 150 °C.

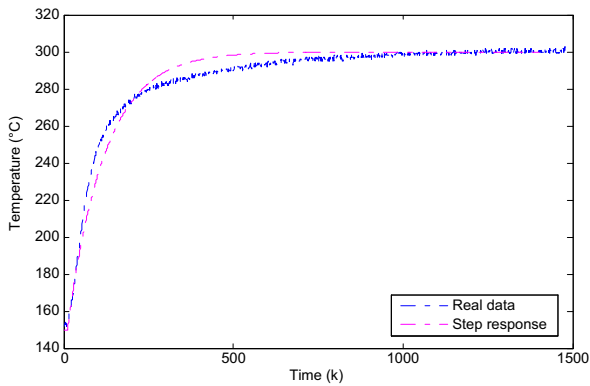


Fig. 6. Step response of the generalized process under the temperature set-point 300 °C.

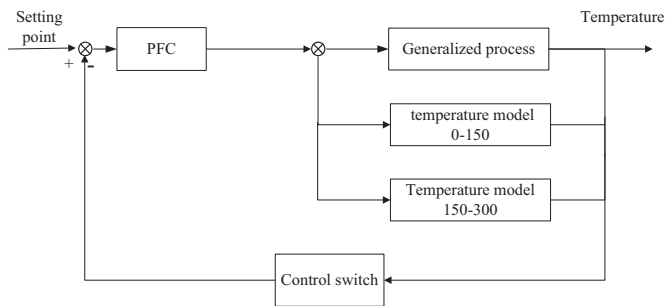


Fig. 7. the block of MMSPFC for heating furnace.

Till now, the step of getting the process models for the different temperature sections is finished. Based on the two different temperature modules, the PFC will be designed. The control structure is shown Fig. 7. Here the prediction horizon is chosen as 40 and the smoothing factor is 0.95. The switch of the models is considered in order to show the effects of model precision. In this experiment, the switch of models will take place according to the temperature value. When the temperature exceeds the current temperature range, the current model will be switched to the next model of the temperature range.

Finally, for comparison purpose, implementation of traditional PFC controller is also investigated and the results are given in the following subsections. The traditional PFC will adopt the same control parameters for a fair comparison.

#### 4.3. Application results

Fig. 8 shows the results of the original PID, the multiple MSPFC and traditional PFC strategies when the temperature set-point is 300 °C. Fig. 9 show the duty ration of solid state relay at every sampling time, which represents the time of heating. We can obtain the corresponding response time of each algorithm from the graph. It takes the MMSPFC about 54 min to drive the temperature to the set-point. Traditional PFC takes about 48 min and the PID takes about 110 min respectively to do so. It seems that traditional PFC will yield a faster speed, however, when the temperature of PFC first reaches the set-point, there will be an overshoot that cannot be eliminated for a very long time. It is shown that there is not such an overshoot in the response of the proposed MSPFC.

In order to compare the steady state property of the two PFC control systems, we collected 1000 sets of data after the system is stable. The results are shown in Fig. 10 and statistical results are further presented in Table 1.

In Fig. 10, it can be seen that the temperature of the process can be maintained at the set-point by both methods. In addition,

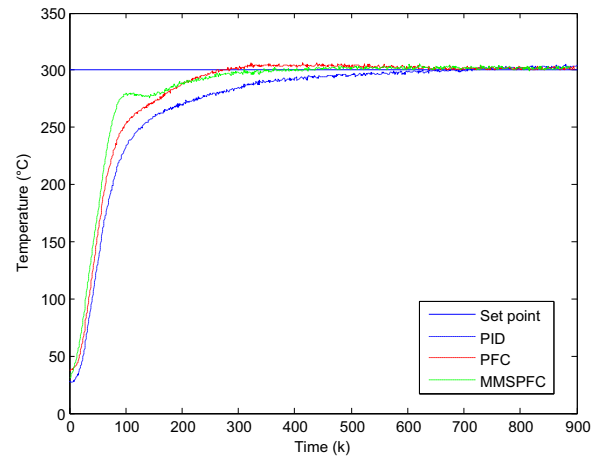


Fig. 8. The performance of the set-point tracking of practical output control.

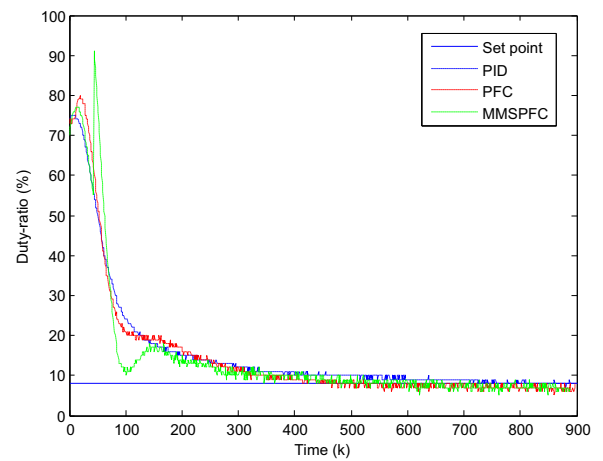


Fig. 9. The duty ration of the set-point tracking of practical input control.

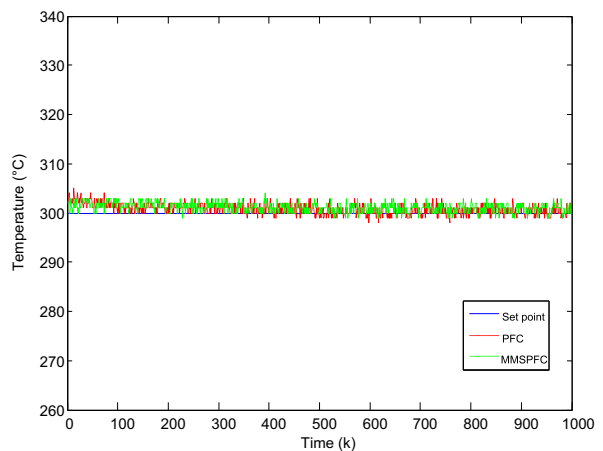


Fig. 10. The steady state performance for practical output control.

Table 1  
Statistical results of steady state performance.

algorithm	Average value	Maximum value	Minimum value	variance	Standard deviation
MSPFC	301.11	303	299	0.969045	0.80593
PFC	300.80	305	298	1.16316	0.8948



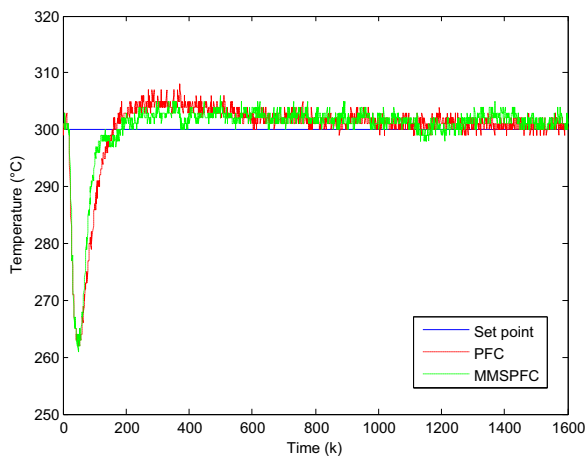


Fig. 11. The disturbance rejection Performance of practical output control.

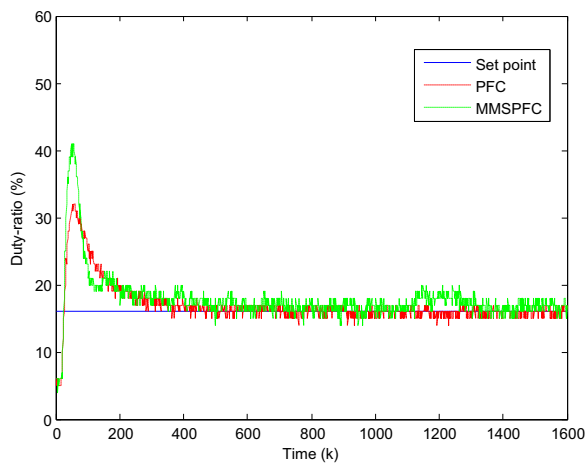


Fig. 12. The disturbance rejection Performance of practical input control.

Table 1 shows more clearly the corresponding statistical results on the average, maximum, minimum, standard deviation and variance of the output temperature. The experimental results show that improved performance will be achieved by the proposed MMSPFC strategy.

The rejection against external disturbance is also a major performance index in process control systems. To verify the control performance under external disturbance, we exerted the disturbance by opening the door of the electric heating furnace to a certain angle when the temperature reaches the steady state. Fig. 11 and Fig. 12 show the temperature responses of the heating furnace and the duty ration of the solid state relay. In Fig. 11, it shows that the proposed MMSPFC and PFC strategy both give the corresponding control action to reject this disturbance and force the temperature to track the required set-point again. It is witnessed that the proposed MMSPFC shows a relatively faster response. The overshoot is smaller compared with traditional PFC.

## 5. Conclusion

A multi-model switching based predictive functional control is proposed in this paper for temperature system of an electric heating furnace. The proposed method combines the advantages

of the PFC with the model switching and improved control results will be obtained in terms of servo and regulatory performance of the closed-loop system.

## Acknowledgment

Part of this project was supported by the National Natural Science Foundation of China (Grant No. 61673147) and Zhejiang Provincial Natural Science Foundation of China under Grant (LR16F030004).

## References

- [1] Trinks W, Mawhinney MH, Shannon RA, Reed RJ, Garvey JR. Industrial furnaces. John Wiley & Sons; 2004.
- [2] Bennett S. Development of the PID controller. *IEEE Control Syst* 1993;13:58–65.
- [3] Ntogramatzidis L, Ferrante A. Exact tuning of PID controllers in control feedback design. *IET Control Theory Appl* 2011;5(4):565–78.
- [4] Shamsuzzoha M, Lee M. IMC-PID controller design for improved disturbance rejection of time-delayed processes. *Ind Eng Chem Res* 2007;46(7):2077–91.
- [5] Zou Q, Jin Q, Zhang R. Design of fractional order predictive functional control for fractional industrial processes. *Chemom Intell Lab Syst* 2016;152:34–41.
- [6] Richalet J, O'Donovan D. Predictive functional control: principles and industrial applications. Springer Sci Bus Media 2009.
- [7] Zhang R, Lu R, Xue A, Gao F. New minmax linear quadratic fault-tolerant tracking control for batch processes. *IEEE Trans Autom Control* 2016;61:3045–51.
- [8] Wu S, Zhang R, Lu R, Gao F. Design of dynamic matrix control based PID for residual oil outlet temperature in a coke furnace. *Chemom Intell Lab Syst* 2014;134:110–7.
- [9] Zhang RD, Xue AK, Gao FR. Temperature control of industrial coke furnace using novel state space model predictive control. *IEEE Trans Ind Inform* 2014;10(4):2084–92.
- [10] Zhang RD, Xue AK, Lu RQ, Li P, Gao FR. Real-time implementation of improved state-space MPC for air supply in a coke furnace. *IEEE Trans Ind Electron* 2014;61(7):3532–9.
- [11] Zhang RD, Li P, Xue AK, Jiang AP, Wang SQ. A simplified linear iterative predictive functional control approach for chamber pressure of industrial coke furnace. *J Process control* 2010;20(4):464–71.
- [12] Manuel GC, Robin DK, Clara I. Nonlinear predictive control with dead-time compensator: application to a solar power plant. *Sol Energy* 2009;83:743–52.
- [13] Liu XJ, Kong XB. Nonlinear model predictive control for DFIG based wind power generation. *IEEE Trans Autom Sci Eng* 2014;11(4):1046–55.
- [14] Vishal M, Juergen H. Model predictive control of reactive distillation for benzene hydrogenation. *Control Eng Pract* 2016;52:103–13.
- [15] Lin CY, Liu YC. Precision tracking control and constraint handling of mechatronic servo systems using model predictive control. *IEEE/ASME Trans Mechatron* 2012;17(4):593–605.
- [16] Zhang RD, Cao ZX, Lu RQ, Li P, Gao FR. State-space predictive-P control for liquid level in an industrial coke fractionation tower. *IEEE Trans Autom Sci Eng* 2015;12(4):1516–24.
- [17] Zhang R, Tao J, Gao F. A new approach of Takagi-Sugeno fuzzy modeling using improved GA optimization for oxygen content in a coke furnace. *Ind Eng Chem Res* 2016;55(22):6465–74.
- [18] Porfirio CR, Neto EA, Odloak D. Multi-model predictive control of an industrial C3/C4 splitter. *Control Eng Pract* 2003;11(7):765–79.
- [19] Kang Y, Zhai DH, Liu GP, Zhao YB. On input-to-state stability of switched stochastic nonlinear systems under extended asynchronous switching. *IEEE Trans Cybern* 2015;46(5):1092–105.
- [20] Chen, H, Li, N, Li, S Y. Switching multi-model predictive control for hypersonic vehicle. In: *8th Asian Control Conference*, 2011; p. 677–681.
- [21] Nandola NN, Bhartiya S. A multiple model approach for predictive control of nonlinear hybrid systems. *J Process Control* 2008;18:131–48.
- [22] Yang H, He LJ, Zhang ZY. Multiple-model predictive control for component content of CePr/Nd counter current extraction process. *Inf Sci* 2016;360:244–55.
- [23] Li SY, Xi YG. Switching smoothly of multi-model predictive control systems. *J Shanghai Jiao Tong Univ* 1999;33(11):1345–7.
- [24] Zeng J, Xue D, Yu, Yuan DC. Multi-model predictive control of nonlinear systems. *J Northeast Univ (Nat Sci)* 2009;30(1):26–9.
- [25] Li N, Li SY, Xi YG. Multi-model predictive control based on the Takagi-Sugeno fuzzy models: a case study. *Inf Sci* 2004;165:247–63.
- [26] Bequette BW. Process control: modeling, design and simulation. Upper Saddle River, NJ, USA: Prentice-Hall; 2003.